A research on the converging process in a T-shape tube

Xi Peng[1, †], Jiarui Yu[2, *, †] and Hongmin Yuan[3, †]

[1]Institute of civil engineering and transportation, South China University of Technology, Guangzhou, Guangdong, 51000, China

[2]Ocean College, Zhejiang University, Zhoushan, Zhejiang, 316021, China

[3]School of Aerospace Engineering, Beijing Institute of Technology, Beijing, 100081, China

*Corresponding author's e-mail: 3180106271@zju.edu.cn

[†]These authors contributed equally.

Abstract. A T-shape tube is an important structure in chemical engineering and other fields. This article utilizes the CFD method on python with a simplified Navier-Stokes equation to stimulate the converging process of different fluids and studies the influence of inflow speed, viscosity, density, diffusion coefficient, the diameter of the tube and the length of the tube on the transmission characteristics like pressure and flow field. The results indicate that the ratio of the velocity of the main tube to that of the branch, the diameter of tube AC and tube B is inversely related with mixing efficiency and that the increase of pipe length at outlet tube and the diffusion coefficient of fluid is positive to the well-distributed concentration of outflow. However, the density and viscosity of inflow seem to have little impact on the mixing process.

Keywords: T-shape tube, Navier-Stokes equation, CFD method.

1. Introduction

Flow transfer pipes are the most important part of engineering structures, which have a wide range of applications in chemical engineering and aerospace engineering [1-4]. T junction is a common type of pipe, which is used in many pipe systems. However, in Chemical engineering, the material of two inlets of T junction may be different, so the mixing situation of two substances at the outlet of the T junction is not clear.

To understand better the process in the T-shape tube, there is already some research about the velocity, pressure, temperature and other transmission characteristics in the tee-pipe or T-shape tube by other scholars [5-8].

Yonghong Duan et al. [5] used Ansys Fluent to examine the turbulent in a 3-dimensional tee pipe and introduced a Segregated implicit method to solve the standard k- £ double equation model. Their results showed that the model could obtain more reasonable and accurate calculation results than other turbulence models.

Lei Cheng et al. [6] utilized CFD (computational fluid dynamics) method to simulate the T-shape tube, and the internal fluid velocity cloud diagram and vector diagram are obtained. They concluded that the fluid flow stability in the pipe would be significantly reduced, the loss to the pipe wall would be large, and even an obvious vortex phenomenon would appear when the inlet velocity of the branch pipe is too large.

Donghua Lu et al. [7] studied a model, which is an equal diameter tee pipe with different fluid temperatures in the main pipe and branch pipe. A numerical simulation was done using AQUA code to analyze the 3-dimensional thermal stratified flow in the tee pipe model. The results showed that the mixing at the converging area is fierce, but the mixing mainly happens downstream of the primary pipe.

Xiaofei Cui et al. [8] made a general stimulation about the velocity and pressure of the inner flow in a T-shape tube using Ansys Fluent and studied the transmission characteristics. They indicated that the inlet velocity distribution and pressure are well-distributed regardless of the pipe diameter and

that the outlet velocity distribution of the t-tee is annular along the axis, while the outlet velocity distribution.

In this research, we simplify the Navier-Stokes equation accordingly, use the method of CFD on python to simulate, and then use the method of controlling variables to study the flow velocity, streamline and concentration diagram of the flow after mixing under different initial conditions. The T-shape tube we used in this research is based on a micro mixer. We also simplified it. We consider the flow between parallel plates, which makes it simple to be simplified into a two-dimensional simulation. Besides, we consider that the flow is without chemical reaction and with different flow directions so that the flow in the T-tube can be mixed without collision.

2. Physical condition

The geometric of T junction is shown in Figure 1. As shown in Figure.1, the main dimension of the T junction is the diameter of the pipe, which is 0.1m. Mixture A and mixture B flow into the pipe from the left and bottom of the T junction and then mix at the intersection of the tube to form sample C.

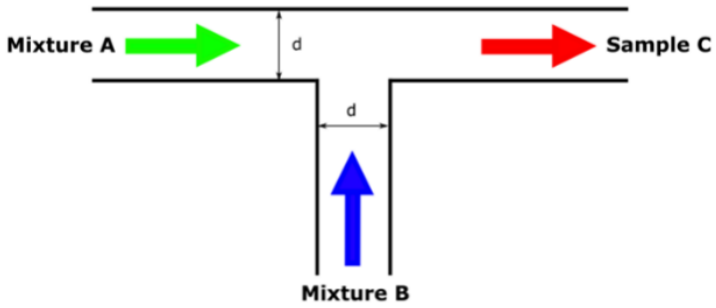


Figure 1. Geometric of T junction

3. Numerical method

The numerical modelling is conducted by typing python code on a jupyter notebook to solve the two-dimensional mass transfer and fluid flow equations according to the following assumptions.

(i) The flow is laminar, incompressible and Newtonian.

(ii) Both fluid flow and heat transfer are in steady-state.

(iii) Neglecting the viscous dissipation and the gravitational force.

(iv) In the present study, the Knudsen number (K_n) is less than (10^{-3}), so the continuum approach based on the Navier-Stokes equations is applicable [9].

According to previous assumptions, the governing equations of mass, momentum, pressure and mass transfer can be written as follows:

Continuity equation:

$$\frac{\partial u}{\partial x}+\frac{\partial v}{\partial y}=0 \tag{1}$$

where u and v are the velocity components in x and y directions, respectively.

Momentum equations:

$$\frac{\partial u}{\partial t}+u\frac{\partial u}{\partial x}+v\frac{\partial u}{\partial y}=-\frac{1}{\rho}\frac{\partial p}{\partial x}+\upsilon\frac{\partial^2 u}{\partial x^2}+\upsilon\frac{\partial^2 u}{\partial y^2} \tag{2}$$

$$\frac{\partial v}{\partial t}+u\frac{\partial v}{\partial x}+v\frac{\partial v}{\partial y}=-\frac{1}{\rho}\frac{\partial p}{\partial x}+\upsilon\frac{\partial^2 v}{\partial x^2}+\upsilon\frac{\partial^2 v}{\partial y^2} \tag{3}$$

where ρ and υ are the density and dynamic viscosity of the fluid, respectively, and p is the fluid pressure.

Poisson pressure equation:

$$\frac{\partial^2 p}{\partial x^2}+\frac{\partial^2 p}{\partial y^2}=-\rho\left(\frac{\partial u}{\partial x}\frac{\partial u}{\partial x}+2\frac{\partial u}{\partial y}\frac{\partial v}{\partial x}+\frac{\partial v}{\partial y}\frac{\partial v}{\partial y}\right) \quad (4)$$

where ρ and p is the density and pressure of the fluid.

Mass transfer equation:

$$N_A=-D_{AB}\left(\frac{\partial c_A}{\partial x}+\frac{\partial c_A}{\partial y}\right)+c_A v \quad (5)$$

$$N_B=-D_{AB}\left(\frac{\partial c_B}{\partial x}+\frac{\partial c_B}{\partial y}\right)+c_B v \quad (6)$$

where N_A and N_B is the mass transfer flux of mixture A and B, respectively and c_A and c_B is the concentration of mixture A and B, respectively. D_{AB} is the diffusion coefficient of mixture A and B, and v is the velocity of the flow.

4. Initial conditions

4.1. Length of the tube at outlet C

In this section, as shown in Table 1, the inlet concentration is fixed for 1 unit, and the concentration for the inlet branch is 0, with the diameter of tube AC and tube B both being fixed for 0.1. Then different pipe length cases are applied to the python code.

Table 1. Initial conditions for different pipe length

Operating condition(OC)	Inlet concentration 1	Inlet concentration 2	Diameter of tube AC&B	Diffusion coefficient	Outlet pipe length
1	1	0	0.1	0.1	15
2	1	0	0.1	0.1	50

4.2. Diffusion coefficient

The initial conditions are similar to that in section 4.1, except that the outlet pipe length is fixed at 15 and that the diffusion coefficient value is the only variable in the equation.

Table 2. Initial conditions for different pipe length

Operating condition(OC)	Inlet concentration 1	Inlet concentration 2	Diameter of tube AC&B	Diffusion coefficient	Outlet pipe length
3	1	0	0.1	0.01	15
4	1	0	0.1	0.1	15

4.3. The flow speed of inlet A&B

Table 3 shows the operating conditions that are applied to the simulation code. Other information includes a model with density for 1000, the diffusion coefficient for 0.001 and different Reynolds numbers depending on the tube's flow speed and diameter.

Table 3. Different operating conditions in 4.3 section

Operating condition	Diameter of AC	Diameter of B	Velocity of A(u_a)	Velocity of B(u_b)
5	150	75	3	3
6	150	75	3	2
7	150	75	3	1
8	150	75	2	3
9	150	75	1	3

4.4. Diameter of tube AC&B

In this research, we change tube AC and tube B (mm) diameters and make other factors constant. The velocity in tubes A and B is 3m/s, the flow density is 1000kg*m^-3, and the viscosity of flow is 0.001kg*m^-1*s^-1. The inlet concentration is fixed for 1 in tube A and for 0 in tube B.

Table 4. Tested value of different diameters of tube AC and tube B in Group 1

Operating condition (OC)	Diameter of tube AC (mm)	Diameter of tube B (mm)	Inlet concentration of tube A	Inlet concentration of tube B
10	2.5	2.5	1	0
11	5	5	1	0
12	7.5	7.5	1	0

Table 5. Tested value of different diameters of tube AC and tube B in Group 2

Operating condition (OC)	Diameter of tube AC (mm)	Diameter of tube B (mm)	Inlet concentration of tube A	Inlet concentration of tube B
13	5	2.5	1	0
14	5	5	1	0
15	5	7.5	1	0

Table 6. Tested value of different diameters of tube AC and tube B in Group 3

Operating condition (OC)	Diameter of tube AC (mm)	Diameter of tube B (mm)	Inlet concentration of tube A	Inlet concentration of tube B
16	2.5	5	1	0
17	5	5	1	0
18	7.5	5	1	0

4.5. Density of flow

In this research, we change the density of flow and make other factors constant. The velocity in tubes A and B is 0.05m/s, the viscosity of flow is 0.001 kg*m^-1*s^-1 and the diameters of tube AC and tube B are 15mm and 7.5 mm.

Table 7. Tested value of flow density

Operating condition (OC)	Density of flow (kg*m^-3)	Diameter of tube AC (mm)	Diameter of tube B (mm)
19	0.6e3	15	7.5
20	0.8e3	15	7.5
21	1.0e3	15	7.5
22	1.2e3	15	7.5

4.6. Viscosity of flow

In this research, we change the viscosity of flow and make other factors constant. The velocity in tubes A and B is 0.05m/s, the flow density is 1000kg*m^-3 and the diameters of tube AC and tube B are 15mm and 7.5 mm.

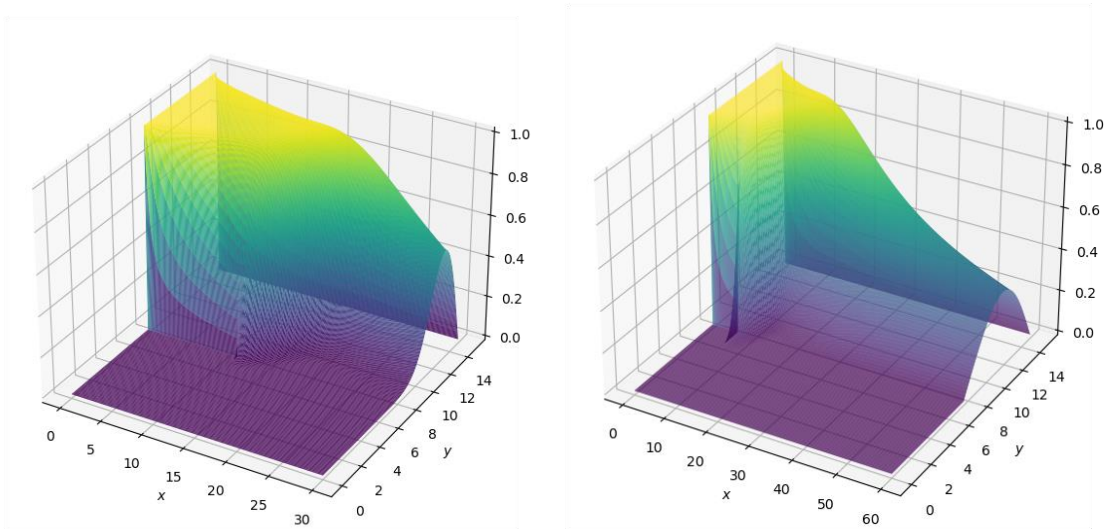
Table 8. Tested value of flow viscosity

Operating condition (OC)	Viscosity of flow (kg*m^-1*s^-1)	Diameter of tube AC (mm)	Diameter of tube B (mm)
23	0.6e-3	15	7.5
24	0.8e-3	15	7.5
25	1.0e-3	15	7.5
26	1.2e-3	15	7.5

5. Results and discussion

5.1. Length of the tube at outlet C

Figure 2 shows the concentration figures for different pipe lengths. Figure 2(a) indicates that the mixing point is at 15 units of tube AC and the whole tube length is 30. After converging, there is a clearly declining trend for the highest concentration and ends up at about 0.4. Figure 2(b) shows the situation when the outlet pipe length is 50. There is a larger declining gratitude near the converging point than Figure 2(a), and then the gratitude becomes smaller. Eventually, the highest outlet concentration is 0.2.



(a) OC1 (b)OC2

Figure 2. Concentration figures for different length cases. (x-axis refers to the length of tube; y-axis refers to the width of the tube; z-axis refers to the value of concentration)

Table 9 shows the stimulation concentration result for different pipe lengths. And with the increase of outlet pipe length, the outlet concentration variance is remarkably declined, which means the mixing process is much better and more efficient. Grbčić et al. [10] did similar research about the mixing assessment of a double-tee junction. The result shows that the concentration was less stratified than the one near the junction, which is in line with our result.

Table 9. Stimulation concentration results for different pipe length

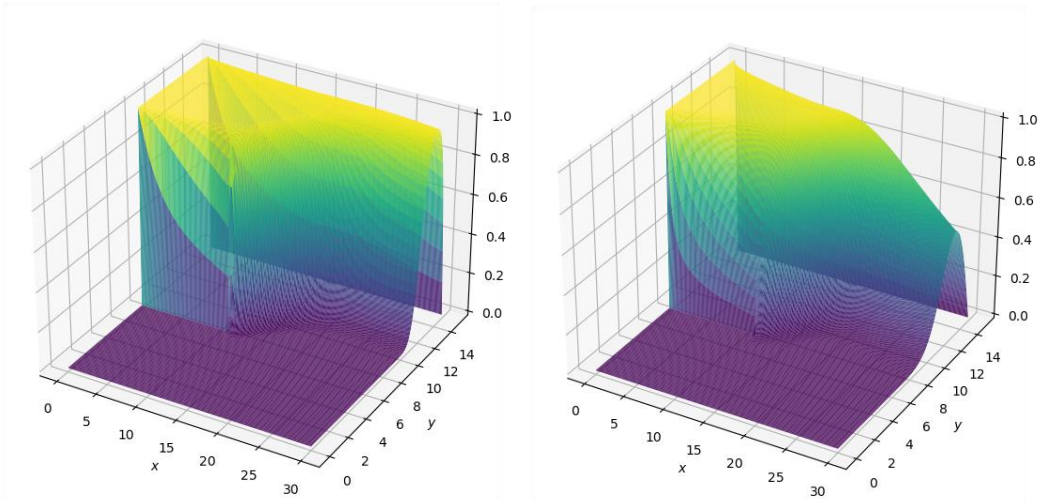
OC	Outlet pipe length	Outlet concentration variance
1	15	0.0355
2	50	0.0112

It can be concluded that a longer tube at outlet C contributes to a better mixing process which means the variance of concentration at the outlet is smaller, thus less stratified and more efficient. Also, given the trend of declining gratitude in Figure 2(b), it is suspected that there has been a unified

trend for the concentration and ending constant concentration depends on the two different inlet fluid and their rate of flow.

5.2. Diffusion coefficient

Figure 3 shows the concentration figures for different 4.2 diffusion coefficient cases. Figure 3(a) shows the result when the diffusion coefficient value is 0.01 and indicates that the fluid is stratified at the outlet with the original high concentration fluid in the middle, low concentration fluid near the boundary and mixing part between the former two areas. And it is noticeable that the highest concentration is still about 1 at the outlet. In Figure 3(b), the highest concentration is still in the middle but declines to 0.4. The low concentration fluid is also near the boundary, but the concentration range is remarkably smaller than when the diffusion coefficient is smaller.



(a) OC3 (b) OC4

Figure 3. Concentration figures for different diffusion coefficient cases

Table 10 shows the stimulation concentration result for different diffusion coefficients. It is suggested that the diffusion coefficient is inversely related to the outlet concentration variance, which is in line with the definition of diffusion coefficient [11].

Table 10. Stimulation concentration result for the different diffusion coefficient

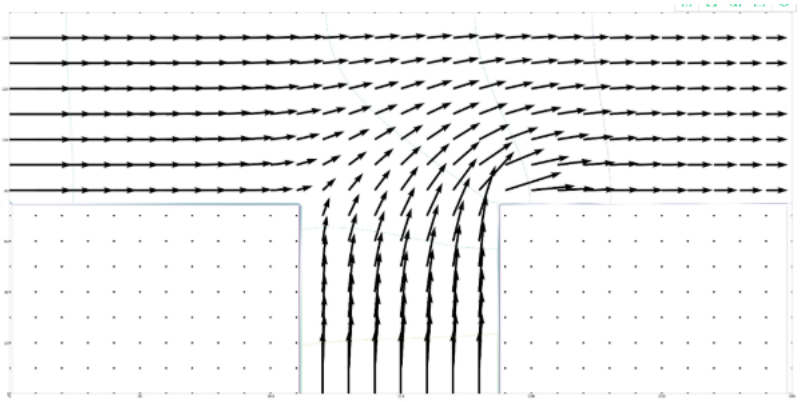
OC	Diffusion coefficient	Outlet concentration variance
3	0.01	0.1553
4	0.1	0.0355

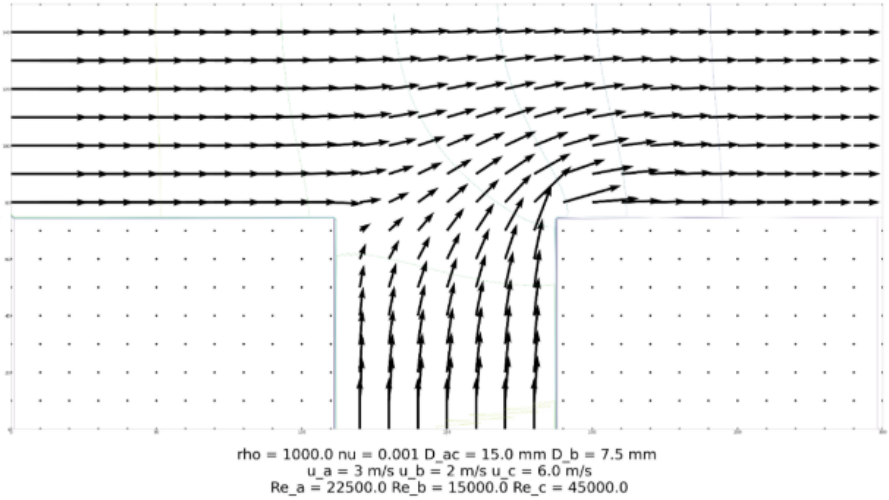
The result indicates that a smaller diffusion coefficient positively influences the mixing process, which means the fluid is well-distributed rather than stratified. Therefore, when designing a converging process in a T-shape tube, the diffusion coefficient of the different fluids had better be small enough to ensure a good outlet flow.

5.3. The flow speed of inlet A&B

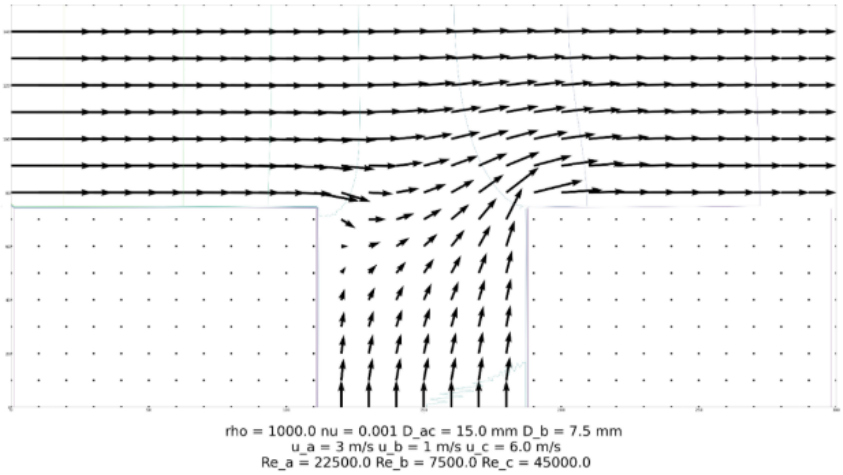
Fig 4 shows the flow field results for different operating conditions. The figures we obtained by python code are in line with the research outcomes by Wang, Y. W et al. [12]. From Fig 4(a), a 45-degree angle of velocity is formed at the junction due to the equal value of two inlet flow speeds. It is noticeable that, given the diameter ratio of tube AC to tube B, the mixing area covers almost a half width of tube AC. Therefore, when u_b is smaller than u_a, as shown in Fig 4(b) and Fig 4(c), the junction's velocity vector angle is smaller. Besides, the left side of the junction in Fig 4(c) indicates that, when u_b is far less than u_a, the flow in tube AC will even go into tube B due to a smaller pressure and then be brought back. And with the decrease of u_b, the mixing area covers a smaller part of tube AC. On the contrary, when u_a is smaller than u_b, as shown in Fig 4(d) and Fig 4(e),

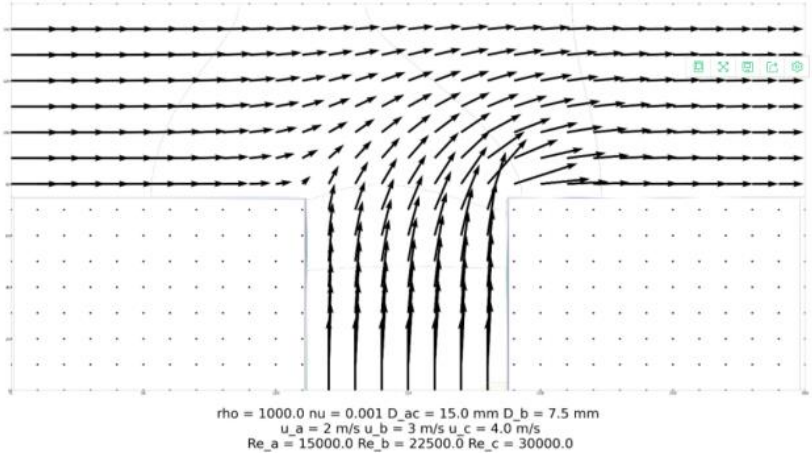
the velocity vector angle is larger than 45 degrees at the junction, and the mixing area covers more than half the width of tube AC.



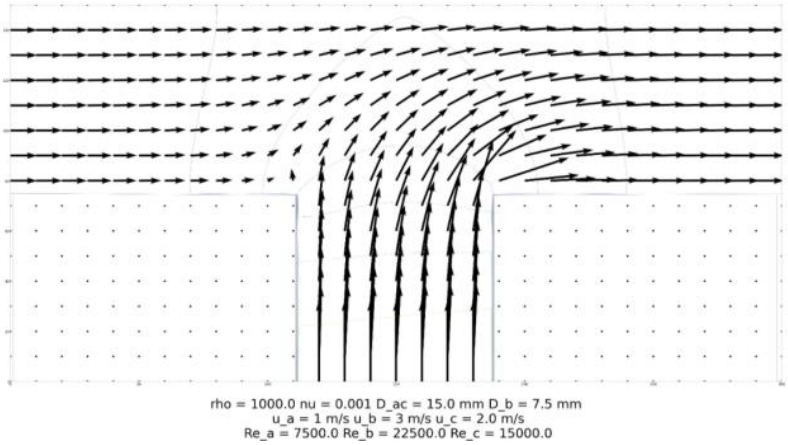


(a) OC5 (b) OC6





(c) OC7 (d) OC8



(e) OC9

Figure 4. Flow field results for different operating conditions

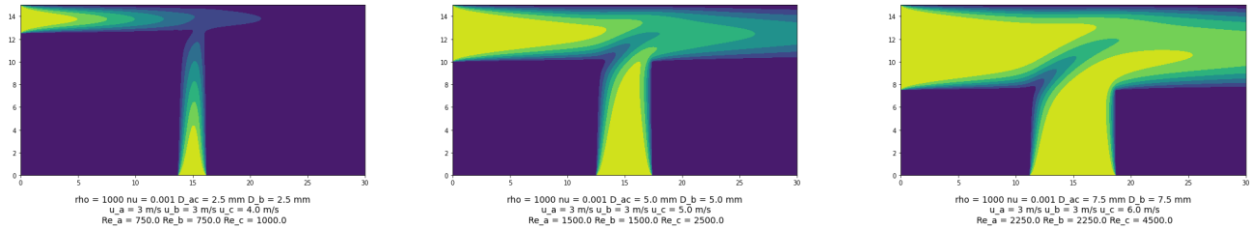
Table 11 shows the stimulation concentration result for different flow speeds of A&B. It can be clearly concluded that with the declining of the u_a to u_b rate, the concentration variance is remarkably suppressed, which can also be explained by Fig 3. When the ratio of u_a to u_b decreases, the mixing area covers a larger part of tube AC which means fiercer converging progress at the junction. However, when the ratio is not small enough, the converging progress is mild, and the flow relies more on the later mixing progress in the outlet tube rather than the junction to become well-distributed, which requires a longer time.

Table 11. Stimulation concentration result for different flow speeds of A&B

OC	Velocity of A	Velocity of B	Variance of concentration
5	3	3	0.0151
6	3	2	0.0353
7	3	1	0.0555
8	2	3	0.0070
9	1	3	0.0018

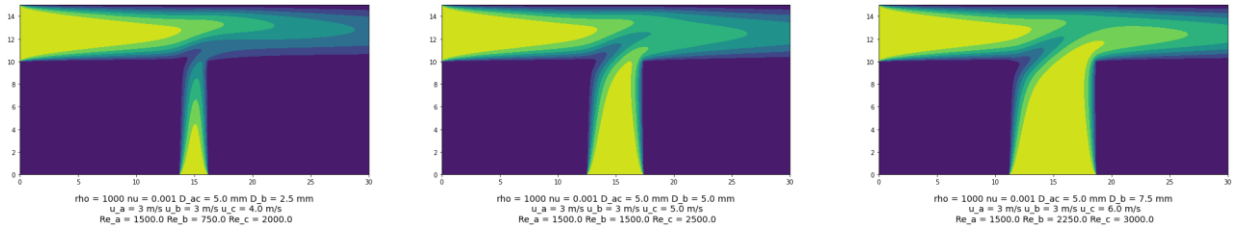
The analysis in this section indicates that a smaller ratio of u_a to u_b contributes to a more efficient mixing T-shape tube due to the smaller variance of concentration. However, in this article, the material of the tube and its pressure are not included. An increase of u_b is sure to augment the pressure on the tube at the junction, thus leading to the damage of the tube. So, a balance of the ratio value should be studied to ensure efficient mixing progress and the protection of tube.

5.4. Diameter of tube AC&B



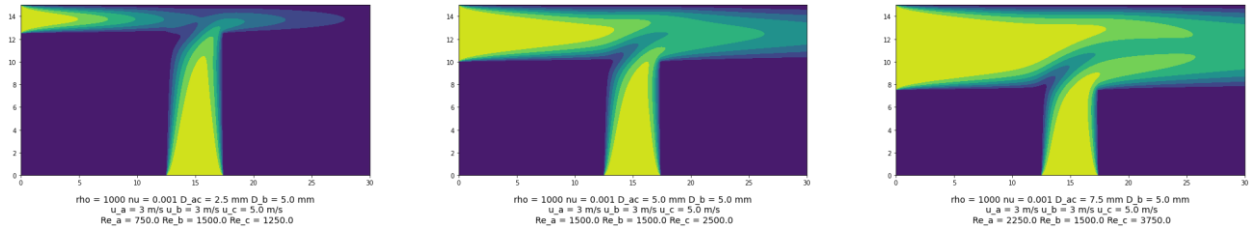
(a) OC10 (b) OC11 (c) OC12

Figure 5. The contour plots of concentration in group 1



(a) OC13 (b) OC14 (c) OC15

Figure 6. The contour plots of concentration in group 2



(a) OC16 (b) OC17 (c) OC19

Figure 7. The contour plots of concentration in group 3

Table 12. The variance of concentration of different diameters of tube AC and tube B in Group 1

Operating condition (OC)	Diameter of tube AC (mm)	Diameter of tube B (mm)	Inlet concentration of tube A	Inlet concentration of tube B	Variance of concentration in tube C
10	2.5	2.5	1	0	0.0464
11	5	5	1	0	0.1410
12	7.5	7.5	1	0	0.1862

Table 13. Variance of concentration of different diameters of tube AC and tube B in Group 2

Operating condition (OC)	Diameter of tube AC (mm)	Diameter of tube B (mm)	Inlet concentration of tube A	Inlet concentration of tube B	Variance of concentration in tube C
13	5	2.5	1	0	0.1113
14	5	5	1	0	0.1410
15	5	7.5	1	0	0.1701

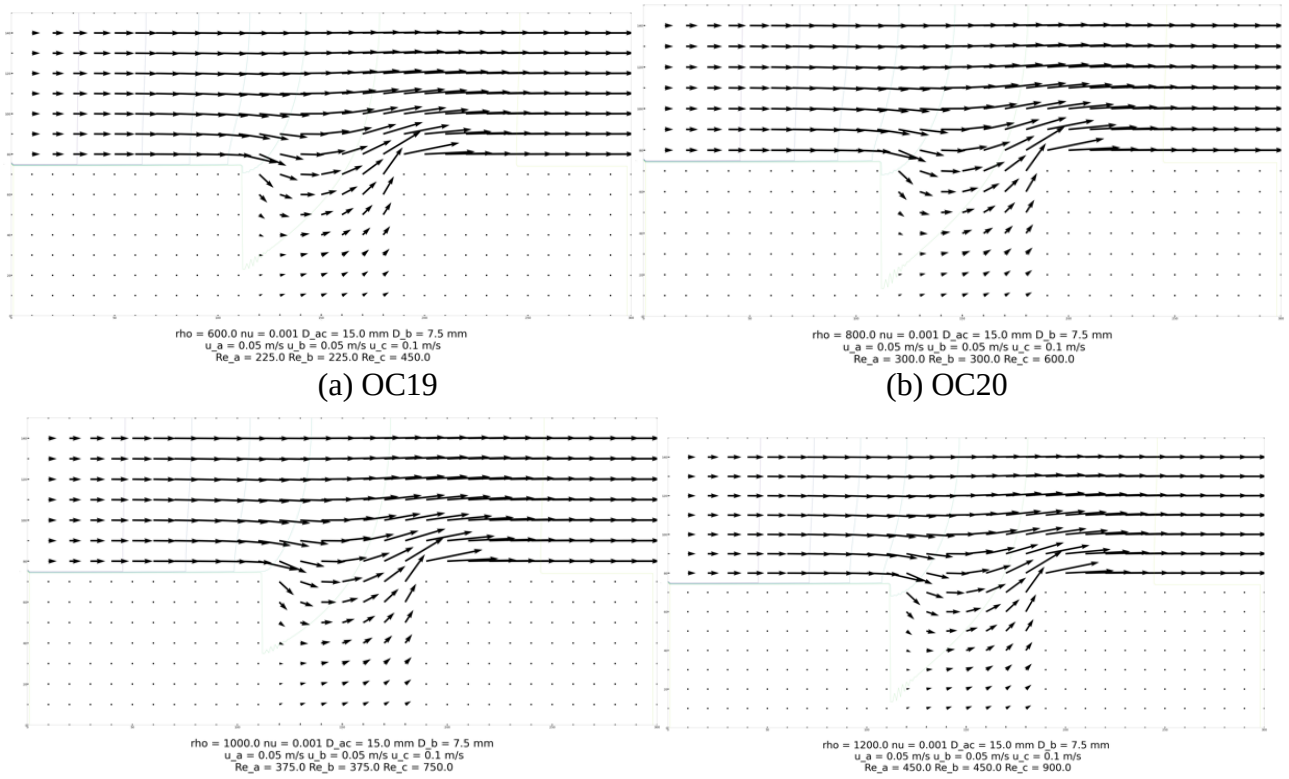
Table 14. Variance of concentration of different diameters of tube AC and tube B in Group 3

Operating condition (OC)	Diameter of tube AC (mm)	Diameter of tube B (mm)	Inlet concentration of tube A	Inlet concentration of tube B	Variance of concentration in tube C
16	2.5	5	1	0	0.0920
17	5	5	1	0	0.1410
18	7.5	5	1	0	0.1736

In Figure 5, if taking the same length of the A and tube B before converging, the concentration with smaller diameters drops faster. Also, the concentration of the tube with larger diameters is more uneven on the right after converging. In Fig 6 if keeping the diameter of tube AC constant, the concentration in tube C is more even when the diameter of tube B is smaller. And these findings were replicated in Group 3. If tube B's diameter constant, the concentration in tube C is more even when the diameter of tube AC is smaller.

The concentration variance in tube C represents the efficiency of mixing, and smaller variance means better mixing. According to Table 12, 13, 14, when the diameters of tube AC and tube B are the same, the mixing efficiency will decrease as diameters increase. Likewise, when the diameter of tube AC or tube B is constant, the mixing efficiency will decrease as the other diameter increase.

5.5. Density of flow



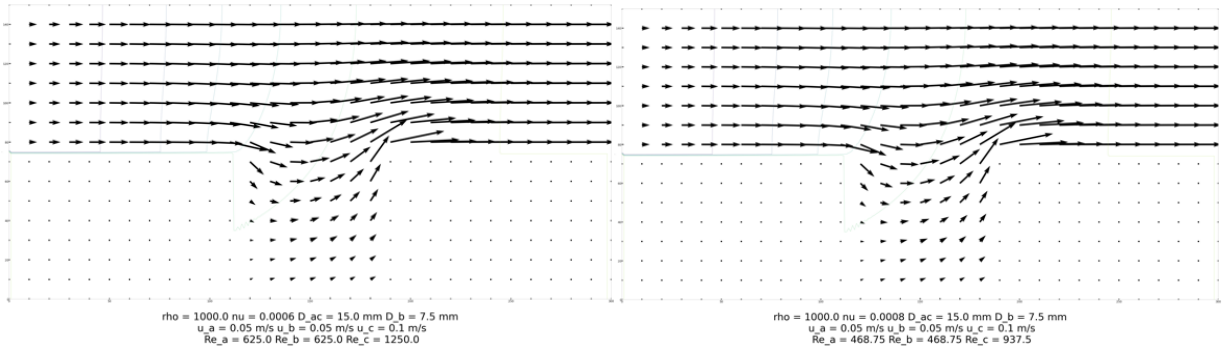
(a) OC19 (b) OC20

(c) OC21 (d) OC22

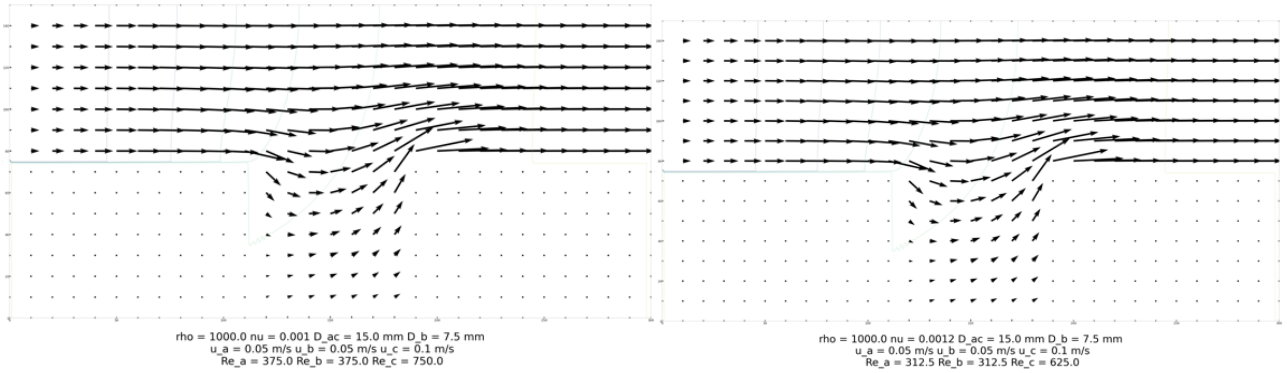
Figure 8. Streamline with different flow density values

According to Fig 8, in the laminar flow statue (Re < 2300), when flow density changes between 800-1200 kg*m^3 (basically liquid), flow speed does not change. As a result, the density of liquid does not influence the speed in the T-shape tube.

5.6. Viscosity of flow



(a) OC23 (b) OC24



(c) OC25 (D) OC26

Figure 9. Streamline with different flow viscosity values

According to Fig 9, in the laminar flow statue (Re<2300), when flow viscosity changes between 0.6*10^-3 - 1.2*10^-3 Pa*s^-1 (basically liquid), flow speed does not change. As a result, the density of liquid does not influence the speed in the T-shape tube.

6. Conclusions

(1) The longer tube at outlet C contributes to a better mixing process. As a result, a unified trend for the concentration and ending constant concentration depends on the two different inlet fluid and their flow rate.

(2) The smaller diffusion coefficient has a positive influence on the mixing process. Therefore, when designing a converging process in a T-shape tube, the diffusion coefficient of the different fluids had better be small enough to ensure a good outlet flow.

(3) Smaller velocity ratio in tube A to velocity in tube B contributes to a more efficient mixing T-shape tube due to the smaller concentration variance.

(4) When the AC tube and B tube diameters are equal, the mixing efficiency will decrease as the diameter increases. When the diameter of one tube is determined, the mixing efficiency will be better if the diameter of the other tube is smaller.

(5) The density and viscosity of liquid do not influence the speed in the T-shape tube.

References

[1] Cheng, K., Liu, C., Guo, T., Wen, L. (2019) CFD and experimental investigations on the micromixing performance of single countercurrent-flow microchannel reactor. Chinese Journal of Chemical Engineering., 27: 1079–1088.

[2] Lun, L.Y., Xie, Y.B., Yang, X.L. (2006) Lng peak shaving proposal based on pressure energy recovery of pipe gas. Natural Gas Industry., 26: 114–116.

[3] Velden, C., Bil, C., Yu, X. (2011) A knowledge-based approach to design automation of wire and pipe routing through complex aerospace structures., Springer London.

[4] Yang, J.H., Sun, J.C., Chen, D.M. (2009) Study on the enhancement of intergranular corrosion properties of 1cr18ni9ti pipe used in aerospace field. Journal of Materials Engineering., 2009: 64–66.

[5] Duan, Y.H., Xu, Q.L., Sun, L. (2008) Three-dimensional numerical simulation of tee-pipe based on Fluent. Inner Mongolia Petrochemical Industry., 2008: 51–53.

[6] Cheng, L., Song, J.L. (2018) Influence of branch pipe flow on fluid velocity field in T-shaped pipe. Guangdong Chemical Industry., 45: 43–44.

[7] Lu, D.H., Toshiharu, M. (2005) 3-D numerical simulation of stripping and stratification in mixing T-junction. Nuclear Power Engineering., 26: 332–334.

[8] Cui, X.F., Cong, X.C., Cao, H.D. (2015) Study on fluid transmission characteristics in T-type tee. Proceedings of 2015 Shandong Annual Academic Conference on HVAC refrigeration and thermal dynamics., 2015: 889–894.

[9] Service, R.F. (1998) Coming soon: the pocket DNA sequencer. Science, 282: 399–401.

[10] Grbčić, L. (2020) Efficient Double-Tee Junction Mixing Assessment by Machine Learning. Water., 12: 238.

[11] Wang, R.X., Qian, C.L., Wang, Y. (2021) Measuring liquid phase diffusivity by observing shift of liquid layer with uniform concentration. Physical Experiment., 2021: 33–38.

[12] Wang, Y.W., Lu, T., Wang, K.S. (2012) Numerical Simulation of Turbulent Flow for Various Inlet Velocities in Tee Junctions with Periodic Porous Media. Advanced Materials Research., 1611: 932–935.